CrossMark

ARTICLE

Engineering star-shaped lactic acid oligomers to develop novel functional adhesives

João M.C. Santos, Diana R.S. Travassos, Paula Ferreira, Dina S. Marques, and Maria H. Gil
CIEPQPF, Department of Chemical Engineering, University of Coimbra, Coimbra P-3030 790, Portugal

Sónia P. Miguel
CICS-UBI, Health Sciences Research Center, University of Beira Interior, Covilhã P-6200 506, Portugal

Maximiano P. Ribeiro
CICS-UBI, Health Sciences Research Center, University of Beira Interior, Covilhã P-6200 506, Portugal; and UDI-IPG-Research Unit for Inland Development, Polytechnic Institute of Guarda, Guarda P-6300 559, Portugal

Ilidio J. Correia
CICS-UBI, Health Sciences Research Center, University of Beira Interior, Covilhã P-6200 506, Portugal

Cristina M.S.G. Baptista[a)]
CIEPQPF, Department of Chemical Engineering, University of Coimbra, Coimbra P-3030 790, Portugal

(Received 30 November 2017; accepted 19 March 2018)

Direct polycondensation of L-lactic acid with a comonomer allows tailoring the properties of the product from the very first step. The viscous L-lactic acid co-oligomers with star-shaped architectures obtained were modified with three different acrylate monomers. Regardless the functionalization agent, UV curing was fast and all materials were cell compatible and promoted cell adhesion. The physical properties of the three star-shaped films exhibited a consistent trend as swelling capacity, hydrolytic instability, and gel content decreased simultaneously. A higher network density increased crosslinking degree and gel content among the films with an isocyanate group. The methacrylic end group functionalized material, lowest molecular weight, consistently exhibited the higher hydrolytic instability. Comparison of physical properties of these films with the corresponding linear materials reported previously confirmed the influence of precursor molecular architecture on the final material. The methodology developed herein is prone to scale-up and lead to the industrial production of new bioadhesives.

I. INTRODUCTION

Polymeric materials with specific functional groups, based on either natural or synthetic substances, are currently broadly used in several biomedical applications. The interest in developing well-tailored bioadhesives has grown exponentially over the past two decades, mainly in areas such as tissue engineering, wound healing, or drug delivery. A surgical adhesive adheres to the tissues or the implants during in situ polymerization and may be used as an alternative to suturing, to control bleeding and to act as a sealant, or even to act as a drug delivery route.[1–5] Despite research efforts, currently available adhesives still have drawbacks, mainly related to toxicity, inflammatory response, and poor adhesiveness under hostile conditions, not to mention the production cost. Ideally, a suitable surgical adhesive must combine an adequate viscosity prior to in situ application, a fast curing rate at physiological temperature, an easy and strong adhesion to tissues, biocompatibility, biodegradability, and good mechanical performance during treatment. The by-products resulting from its degradation in moist environments should be gradually metabolized in the body without eliciting inflammatory responses.[1–4]

The utilization of photocurable polymers as surgical adhesives is very attractive due to the advantages of photopolymerization over other initiation mechanisms. These advantages include short UV exposure time, low energy requirements, and low cost.[3,5–8] Additionally, a great asset of such UV sensitive systems is allowing the adhesive to cure almost instantaneously, however selectively, in strongly illuminated areas such as the operating rooms.[9] Among the plethora of polymers currently available, photocurable polysaccharides (e.g., chitosan, starch, or dextran), aliphatic polyesters, their copolymers and polyethylene glycol (PEG)-based formulations, have been considered the most promising raw materials for producing surgical adhesives, mainly due to their biocompatibility and for being hydrolysable under wet conditions.[10–13] However, polysaccharide and PEG-based adhesives considerably swell up after in vivo application, compromising their mechanical properties and thus hindering a good adhesion.[14,15]

[a)]Address all correspondence to this author.
e-mail: cristina@eq.uc.pt
DOI: 10.1557/jmr.2018.73

https://doi.org/10.1557/jmr.2018.73 Published online by Cambridge University Press

 © Materials Research Society 2018

Poly(lactic acid) (PLA) has emerged as one of the most auspicious man-made polymers for a wide range of biomedical end-uses.[16,17] Previously, we reported the synthesis of linear lactic acid-based oligomers through distillation and self-condensation of L-LA with 1,4-butanediol.[18–20] These oligomers were then functionalized with different photosensitive molecules—methacrylic anhydride (MAA), LAROMER® LR 9000 (LAR), and 2-isocyanatoethyl methacrylate (IEMA)—and their potential suitability as bioadhesives was assessed.

Based on the previously obtained results, as well as on the work reported by other authors,[21,22] star-shaped lactic acid oligomers were prepared and their performance was compared with those of linear oligomers.[23] From the wide range of polyols available, pentaerythritol (mPET) was selected for this new study since it is a versatile building block suitable to manufacture several functional compounds, which is biodegradable and environment friendly.[24] With four terminal hydroxyl groups, it enables tuning monomer/comonomer ratios to determine the viscosity of the L-LA telechelic prepolymers, as well as designing some properties of the polymeric network such as swelling degree, hydrolytic degradation, and thermal stability.[22] The carboxyl groups of L-LA will react preferentially with the primary OH-end groups of mPET, being mPET the core of the resulting star-shaped prepolymer. The synthesized oligomers were then reacted with functionalized molecules obtaining macromers that could be fast photocured. For these reasons, other authors have reported the synthesis of star-shaped lactic acid oligomers using mPET as well as described the suitability of these biobased resins as coatings.[25]

From the diversity of functional agents with free carbon double bonds available, MAA, LAR, and IEMA were tested. MAA has been previously used to modify polyesters (e.g., PLA and polycaprolactone) aimed to be applied in different biomedical applications, particularly for short-term applications.[7] This compound is highly reactive with the hydroxyl groups of the copolymer chains (at high temperature and by direct condensation).[18] Toxicity concerns were minimized as catalysts were avoided and the reactions do not require the use of solvents. Additionally, the hydrophilic nature of the compound may contribute to increase the hydrolysis trend of the final networks. Furthermore, the modification of lactic acid prepolymers with isocyanate compounds (IEMA) provides an adjacent urethane segment. The urethane moiety allows for hydrogen bonding improving the mechanical properties and adhesion of the final networks. In recent years, IEMA has exhibited some promising features for the development of a diversity of tissue adhesives and drug delivery systems.[13,26–28] Moreover, several studies have confirmed that the addition of a low concentration of IEMA does not compromise the biocompatibility of the final materials. On the other hand, LAR presents other interesting features like two carbon double bonds and two terminal isocyanate groups, which besides being capable of reacting with the OH end groups allow testing different oligomer/LAR ratios thus enabling the tuning of the products' final properties. According to the BASF reports, the use of this compound originates materials with improved strength, flexibility, and adhesion to surfaces.

Finally, a biocompatible photoinitiator (e.g., Irgacure® 2959) was added to the synthesized star-shaped macromers that under UV light irradiation originated flexible films. To evaluate the suitability of the synthesized materials to the pretended biomedical application, their chemical and thermal properties as well as their biological performance were assessed.

II. EXPERIMENTAL

A. Materials

L-lactic acid solution (80% v/v), mPET (99%), MAA, IEMA, diethyl ether, and phosphate-buffered saline solution (PBS) were purchased from Sigma-Aldrich (Sintra, Portugal) and used without further purification. LAROMER® LR 9000 and Irgacure® 2959 were kindly provided by BASF.

Glutaraldehyde solution was acquired from Acros organics (Jersey City, New Jersey). 3-(4,5-dimethylthiazol-2-yl)-5-(3-carboxymethoxyphenyl)-2-(4-sulfophenyl)-2*H*-tetrazolium (MTS)/phenazine methosulfate (PMS) was bought from Promega (Canada, USA). Normal Human Dermal Fibroblast (NHDF) cells were purchased from PromoCell (Labclinics, S.A., Barcelona, Spain). Ethanol (EtOH, 90%) was bought from José Manuel Gomes dos Santos (Odivelas, Portugal). All other chemicals used were of reagent grade and were used as received.

B. Synthesis procedures

1. Step 1—production of tailor-made star-shaped co-oligomers

Commercial lactic acid solution of the L-isomer (L-LA) (80% v/v) was the prime monomer in this study. First, L-LA monomers were polymerized by direct esterification with mPET in the absence of catalysts or solvents. The reactions were carried out under melt conditions, at atmospheric pressure, in a two-neck round-bottom glass flask.

Approximately 100 mL of an 80% (v/v) solution of L-LA (equivalent to 96.72 g of monomer) were introduced in the round-bottom glass flask equipped with a magnetic stirrer and connected to a glass condenser. According to the reaction stoichiometry and target molecular weight, 18.24 g of mPET (0.134 mol) were added to the same flask that was then immersed in a heating bath at 150 °C for 9 h. A continuous nitrogen

https://doi.org/10.1557/jmr.2018.73 Published online by Cambridge University Press

gas flow was maintained during the reaction period to guarantee an inert atmosphere. Once the reaction was complete, the flask was removed from the heating bath, and after cooling, the low-viscosity oligomer (star_oligLA) was properly stored in a desiccator for further functionalization.

2. Step 2—functionalization with acrylic monomers

Three functional agents containing vinyl groups MAA, IEMA, and LAR were assessed to functionalize the star_oligLA. Experimental procedures for each case will be briefly described. All the reactions were conducted in a round bottom flask immersed in an oil bath and under an inert atmosphere. Diethyl ether was used as the solvent (5–10 mL). Therefore, the reaction flask was coupled to a glass condenser attached to a drying tube filled up with calcium chloride to reflux the solvent.

To modify both ends of the star_oligLA chains, 1 mol of MAA was added per 2 mol OH end groups, assuming that the methacrylic acid resulting from the reaction is also consumed.[18] This reaction was conducted at 130 °C for the period of 24 h under constant magnetic stirring. In the IEMA reactions, a proportion of 4 mol of IEMA per mole of star_oligLA was used to modify all the OH groups by reaction with isocyanate groups. For the reaction with LAR, the optimized molar ratio of NCO/OH groups was 1/1, aiming at obtaining highly flexible materials. Each reaction was carried out under constant magnetic stirring and at 60 °C, for 24 h for IEMA and for 4 h when LAR was the functional agent. Optimal times were established by Attenuated total reflectance–Fourier transform infrared spectroscopy (ATR–FTIR) analyses throughout reaction periods.

3. Step 3—production of photocurable networks

Irgacure® 2959 was added (1% of the C=C moles) to all copolymer mixtures and stirred for homogeneity, at 60 °C and under reflux, protected from light. Lastly, transparent and highly flexible adhesives were produced using UV irradiation for 120–180 s. A multiband UV/VIS irradiation chamber was used (model BS-02 from Dr. Gröbel UV-Elektronic GmbH, wavelengths 100–320 nm). All materials were properly dried overnight under vacuum conditions, at room temperature, before characterization.

The synthesis path of all networks herein reported, steps 1–3, is outlined in Fig. 1. The nomenclature of each product is also exhibited.

C. Characterization techniques

Several properties of the star-shaped networks were evaluated to study their potential as photocurable bioadhesives.

1. ATR–FTIR

ATR–FTIR was used to monitor the synthesis steps and curing reactions by identifying the reaction products. The spectra were recorded on a Jasco FT/IR-4200 spectrometer (Jasco, Tokyo, Japan) equipped with a Golden Gate single reflection diamond ATR at an average of 128 scans, with a resolution of 4 cm^{-1}.

2. Gel content

The materials gel content was determined by solvent extraction. Samples of dried films were weighed (W_0) and immersed in diethyl ether overnight in sealed containers. The samples were later removed and dried under vacuum until reaching constant weight (W_1). Gel content was determined as shown in Eq. (1).

$$\text{Gel content } (\%) = W_1/W_0 \times 100 \quad . \qquad (1)$$

3. Swelling capacity

Samples of each film were carefully dried under vacuum before the tests and weighed (W_d). The samples were placed in a container with a saturated solution of pentahydrate copper sulfate at room temperature. At predetermined times, the samples were reweighed until maximum weight was reached (W_s). The study was performed in triplicate. The swelling capacity was determined by Eq. (2):

$$\text{Swelling capacity } (\%) = (W_s - W_d)/W_d \times 100 \quad . \quad (2)$$

4. Hydrolytic instability

Dried film specimens (1 mm thickness) were weighed ($W_{d,0}$), immersed in 10 mL of PBS (0.01 M; pH = 7.4), and submitted to hydrolytic degradation for six weeks, at 37 °C. At predetermined times, the samples were removed from PBS, washed with distilled water, and dried under vacuum until reaching constant weight ($W_{d,t}$). The degree of degradation was estimated from the weight loss, which was calculated using Eq. (3):

$$\text{Weight loss } (\%) = \left(W_{d,0} - W_{d,t}\right)/W_{d,0} \times 100 \quad . \quad (3)$$

5. Thermal properties

Dynamic Mechanical Thermal Analysis (DMTA) measurements of thick network samples were performed using a Triton Tritec 2000 (Triton Technology, Ltd., Grantham, United Kingdom) under the tensile and multifrequency conditions (1 and 10 Hz), with a typical heating rate of 5 °C/min. Glass transition temperature, (T_g), was considered as the peak in tan δ at 1 Hz.

6. Characterization of the cytotoxic profile of the films

The cytotoxic profile of the films was evaluated through in vitro assays. NHDFs were used as model cells and seeded in direct contact with the films, as

https://doi.org/10.1557/jmr.2018.73 Published online by Cambridge University Press

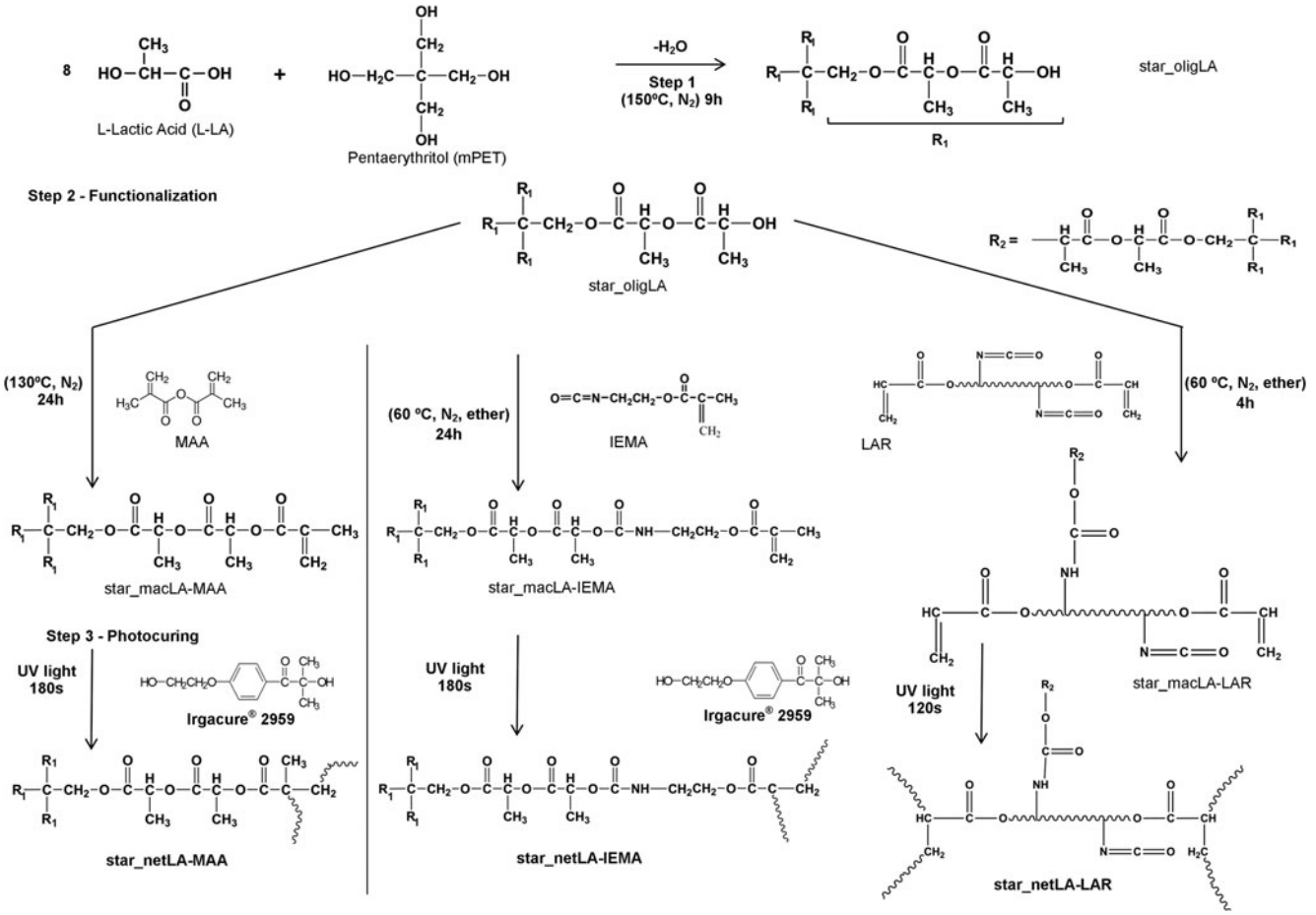


FIG. 1. Schematic representation of the star-shaped oligomers synthesis, functionalization, and crosslinking reactions; together with nomenclature.

previously described elsewhere.[18–20] Briefly, 10×10^3 NHDF cells were seeded per well and incubated at 37 °C, in a 5% CO_2 humidified atmosphere. After 1, 2, 3, 7, 10, and 14 days of incubation, an MTS assay was performed to characterize cell metabolic activity. Then, the culture medium was removed and replaced by a mixture of 100 μL of fresh culture medium and 20 μL of MTS/PMS reagent solution, and subsequently plates were incubated for 4 h, at 37 °C, in a 5% CO_2 atmosphere. Afterward, the absorbance of each well was determined at 492 nm using a microplate reader (Biorad xMark microplate spectrophotometer, Bio-Rad, Hercules, California). Five replicates of each sample were analyzed. Cells cultured without materials were used as a negative control (K^-), whereas cells in contact with EtOH 90% were used as a positive control (K^+). Furthermore, cell proliferation was also monitored by using an Olympus CX41 inverted light microscope (Olympus, Tokyo, Japan) equipped with an Olympus SP-500 UZ digital camera (Olympus, Tokyo, Japan).

7. Live/dead assay

Cell viability and proliferation at the surface of the films were evaluated by fluorescence microscopy through live/dead assay (Invitrogen, Life Technologies, Foster City, CA). This method allows the simultaneous detection of both live and dead cells with calcein acetoxymethyl (calcein AM) and propidium iodide dyes. Calcein AM is a nonfluorescent and permeable reagent, which is converted by the intracellular esterases into an intense green fluorescent calcein (ex/em: ~495 nm/~515 nm). Propidium iodide is a popular red-fluorescent nuclear probe that only enters into cells through damaged cell membranes (ex/em: 493 nm/~636 nm).[29]

To perform the assays, NHDF cells (10×10^3 cells/mL) were seeded on the surface of the films, which were previously placed in μ-Slide 8 well Ibidi imaging plates (Ibidi GmbH, Planegg/Martinsried, Germany). Cells cultured without materials were used as a negative control (K^-), whereas cells treated with permeabilization solution were used as positive control (K^+). After 1, 2, and 3 days, the cells were incubated with the staining solution, prepared according to the manufacturer's instructions, for 15–20 min. After that, the stained cell cultures on the films were analyzed by fluorescence microscopy and images were captured using Zeiss Zen 2010 software (Zeiss, Oberkochen, Germany).

https://doi.org/10.1557/jmr.2018.73 Published online by Cambridge University Press

8. Characterization of cell adhesion and proliferation on the films' surface by scanning electron microscopy

The bioadhesive properties of the produced films were evaluated by scanning electron microscopy (SEM), using a procedure previously described elsewhere.[30] To accomplish that, NHDFs (of 20×10^3 cells per well) were seeded at the surface of the films. After 1, 2, and 3 days of incubation, the films and their adherent NHDFs were fixed with a glutaraldehyde solution [2.5% (v/v)] and then dehydrated in graded EtOH of 70, 80, 90, and 100% (v/v). Later, the samples were dried under supercritical conditions and mounted on an aluminum stub with Araldite glue and sputter-coated with gold using a Quorum Q150RES sputter coater (Quorum Technologies Ltd., Laughton, United Kingdom). SEM images were acquired with different magnifications, using an acceleration voltage of 20 kV, on a Hitachi S-3400N scanning electron microscope (Hitachi, Tokyo, Japan).

III. RESULTS AND DISCUSSION

A. Synthesis and ATR–FTIR analyses

The experimental synthesis path herein reported, which may be revisited in Fig. 1, enabled obtaining three different photocrosslinked materials. Making use of a star-shaped comonomer (mPET) and based on a solvent and catalyst free process, L-lactic acid was submitted to thermal dehydration, yielding low molecular weight prepolymers with four OH terminal groups. Afterward, these prepolymers (referred as star_oligLA) were modified with three distinct functional agents (MAA, IEMA, and LAR) to introduce photocurable sites in the polymer chains. Experimental procedures were designed in accordance with the functional agent and previous experience with this type of reactions. All macromers (star_macLA-MAA, star_macLA-IEMA, and star_macLA-LAR) showed a viscous oily appearance with potential for in situ injection use. To cure instantaneously under mild conditions, a biocompatible photoinitiator well known in the biomedical field (Irgacure® 2959) was dissolved in all macromers. After UV irradiation for about 120–180 s, flexible and transparent films were manufactured and underwent characterization to evaluate their properties. Since we recently reported several lactic acid adhesives based on a linear-shaped precursor,[18–20] a comparison of overall performances is to be highlighted throughout this work.

First, the success of reactions throughout this three-step approach was monitored by ATR–FTIR (Fig. 2) establishing optimal reaction times at 4 h for the modification with LAR, and at 24 h for the other two functional agents. The ATR–FTIR spectra in Fig. 2: (a) L-LA and co-oligomer, (b) functional agents, (c) macromers, and (d) films were grouped according to the synthesis sequence shown in Fig. 1. Examining Fig. 2(a), the main difference between the spectra lies in the hydroxyl stretching peak which for L-LA solution is at 3378 cm^{-1} and is also shown in the star_oligLA spectrum at 3438 cm^{-1}, but not as sharp. This may be ascribed to the loss of water during polycondensation reactions at fairly high temperature, 150 °C, until obtaining a dried viscous oligomer with potential for modification with functional monomers. The ester linkages, corresponding to C=O elongation, are shown in the L-LA spectrum, at 1738 cm^{-1} and in every spectra in Figs. 2(a), 2(c), and 2(d), as expected. Hydroxyl stretching at 3438 cm^{-1} in the star-oligLA faded away after every functionalization [as can be seen in Fig. 2(c)]. For star_macLA-MAA and star_macLA-IEMA, carbon double bond stretching appeared at 1636 cm^{-1}. On the other hand, the same double bonds were registered at 1686 cm^{-1} for star_macLA-LAR. These wave numbers are in agreement with the C=C stretches for the corresponding functional agents [Fig. 2(b)]. Urethane segments were detected at ~1540 cm^{-1} in the copolymers modified with isocyanate compounds [Fig. 2(c)], while the peaks matching free isocyanate groups (~2260 cm^{-1}) did not show, confirming their full conversion in urethane groups by reaction with the polyol end groups. Moreover, the band corresponding to star_oligLA hydroxyl groups [Figs. 2(a) and 2(c)] disappeared in the macromer spectra, allowing concluding that OH end groups aplenty reacted with the NCO groups. Similarly, for the product modified with MAA [Fig. 2(c)], the peak corresponding to anhydride bonds was not detected in the functionalized prepolymer, therefore confirming the reaction success. After UV irradiation, the disappearance of the double bond stretching in the ATR–FTIR spectra of the networks [Fig. 2(d)] is a consequence of photocrosslinking. Curing time was set at 180 s for MAA and IEMA modified macromers and at 120 s for the ones modified with LAR. This may be due to the double bond density of this functional agent.

Considering process conditions described before, the required curing times and taking into account the results obtained for the linear-shaped products developed before, one can conclude that, among the three functional agents assessed, LAR is the more cost-effective for the production of enhanced photocurable materials for surgical needs. In both types of products (linear[20] or star-shaped), only 4 h were needed to produce a modified lactic acid prepolymer, and well-defined and uniform films were obtained after UV irradiation for 120 s. For the other functional agents, 24 h were required to reach full conversion of the functional monomer. Furthermore, the curing time was extended to 180 s for the star-shaped MAA and IEMA macromers. This may be attributed to the branched structure of these macromers, and a higher density of carbon double bonds in the final products, which may require more time of UV exposure to

https://doi.org/10.1557/jmr.2018.73 Published online by Cambridge University Press

crosslink these samples. Despite the differences, all lactic acid-based materials produced by using this simple three-step production strategy exhibited fast curing rates suitable for in situ applications.

In Sec. III.B–III.G, the main properties of the star-shaped materials summarized in Table I will be presented, highlighting that the different reactive polymer terminal groups contribute to distinct film behaviors.

B. Gel content

The crosslinking degree of the films may be assessed by measuring gel content and it is expected to depend on the functional agent used. The number of carbon double bonds differs between the three macromers as shown in Fig. 1, therefore influencing the crosslinking degree of films.[22] Gel content results displayed in Table I confirm this, as star_netLA_LAR has the higher value (95%). This pattern was also registered for the films prepared with linear oligomers, where the ones modified with LAR showed a 95% gel content, a significant higher value than the ones modified with IEMA (gel content of 89%) and with MAA (gel content of 77%). This property is also dependent on the molecule architecture (linear or branched) and an expected increase in gel content was registered in the star-shaped films.

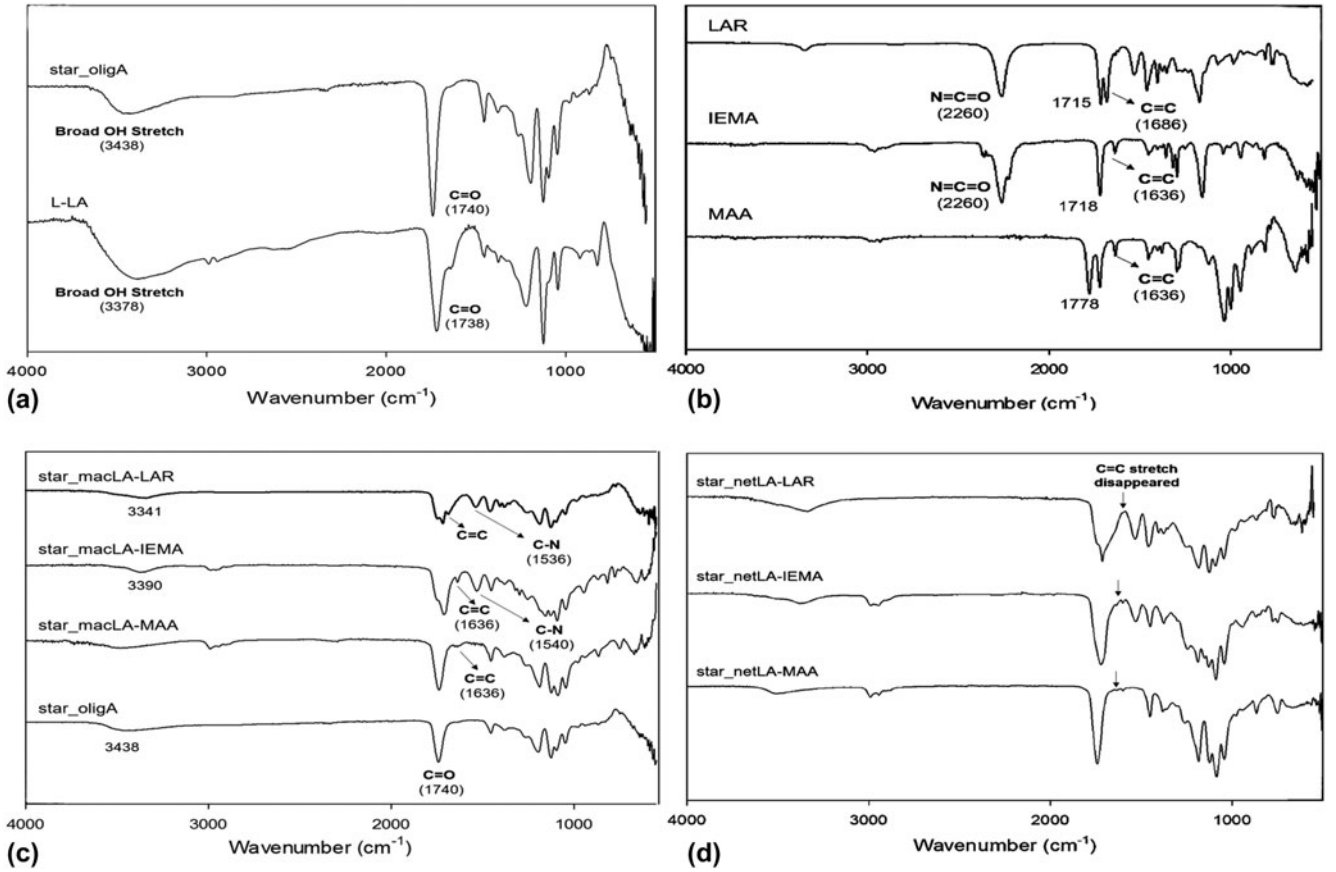


FIG. 2. ATR–FTIR spectra: (a) L-lactic acid and star_oligLA; (b) Functional agents—MAA, IEMA, and LAR; (c) Macromers—star_macLA-MAA, star_macLA-IEMA, and star_macLA-LAR; (d) Networks—star_netLA-MAA, star_netLA-IEMA, and star_netLA-LAR.

TABLE I. Characterization of the star-shaped films produced.

Properties	star_netLA-MAA	star_netLA-LAR	star_netLA-IEMA
M_n target macromers (g/mol)	984	1868	1332
Curing time (s)	180	120	180
Swelling (%) PBS medium	28.7 ± 9.3	16.1 ± 3.1	5.9 ± 3.0
Gel content (%)	...	95	91
Hydrolytic instability % weight loss in 6 weeks	42.3	38.2	15.6
T_g (°C) DMTA measurement	15	13	11
Cell viability	99	97	90
Visual appearance	Yellowish and flexible	Transparent, very resistant, and flexible	Transparent and very flexible

https://doi.org/10.1557/jmr.2018.73 Published online by Cambridge University Press

C. Swelling capacity and hydrolytic instability

Bioadhesives, based on either natural or synthetic raw materials, can detach from or be absorbed by the body, when no longer needed. For internal uses, biodegradability is a crucial feature. L-LA–based films are expected to be quite susceptible to hydrolytic degradation due to the hydrolysis weakness of the ester bonds in the lactic acid oligomer precursors. The degradation process is therefore strongly influenced by the swelling behavior of the polymer matrix, an important feature to guarantee when short-term applications are envisioned. On the other hand, the absorption capacity of the networks and subsequent increase in volume are important parameters to take into account since in surgical adhesives, swelling should be moderate not to damage the surrounding tissues. The results obtained for the hydrolytic degradation of films and their swelling behavior are illustrated in Fig. 3. As can be observed, all star-shaped materials present hydrolytic instability. All samples underwent a substantial weight loss in the first days of the experiment, followed by a slower process over time. Some of the initial weight loss may be attributed to the release of low molecular weight compounds, such as residual monomer, photoinitiator molecules trapped in the networks, or even traces of solvent. Considering the data in Fig. 3 and the performances of the linear-based films previously reported,[18–20] it can be inferred that weight loss is strongly dependent on the structure of the prepolymer, the functional comonomer, the molecular weight, the crosslinking degree, the glass transition temperature, and the swelling capacity. The same results were obtained when working with linear oligomers,[18–20] where, for a six-week experiment, registered weight loss values were of 40.8, 17, and 27.1% for the films prepared with oligomers based on MAA, LAR, and IEMA, respectively.

Considering the films prepared with star-shaped oligomers, the star_netLA-IEMA film exhibited the lowest degradation rate, with a weight loss of around 15% at the end of the six-week experiment. The urethane segments are known as hydrophobic structures and this feature, combined with the density of the network due to high crosslinking, may jeopardize the swelling capacity of the material, hindering a faster degradation. According to Hakala et al.[22] and Makadia et al.,[31] polymers with higher swelling exhibit higher rates of hydrolytic degradation. This may explain the decrease in hydrolytic instability when comparing the star-shaped films (MAA > LAR > IEMA) in Table I.

LAR and IEMA are both isocyanate compounds and unexpectedly, according to the results shown in Table I, the star_netLA-LAR films revealed a very fast hydrolytic degradation rate compared to star_netLA-IEMA. The main explanation for this result may lie on the molar ratio used to modify the star-shaped lactic acid prepolymer. The branched structure with many free OH terminal groups led to a substantial increase in the swelling capacity of the networks and thus an increase in the mass loss.

The hydrolytic degradation profiles of the star_netLA-MAA and star_netLA-LAR films were very similar (Fig. 3) despite MAA being an anhydride. The higher degradation rate of the star_netLA-MAA may be mainly explained by the swelling capacity of this material (~29%). According to Seppälä et al.[7] and Hakala et al.,[22] polyesters modified with anhydride compounds exhibit a two-stage degradation mechanism (usually initiated by surface erosion) due to hydrolytically labile anhydride bonds, which leads to a fast degradation rate. Furthermore, when the samples are incubated in an aqueous medium, acidic degradation products (such as methacrylic acid species) will be accumulated in the surrounding medium. The buildup of these degradation products might catalyze the hydrolysis reactions.

It is important to keep in mind that these results concern in vitro incubation. Previous studies have proven

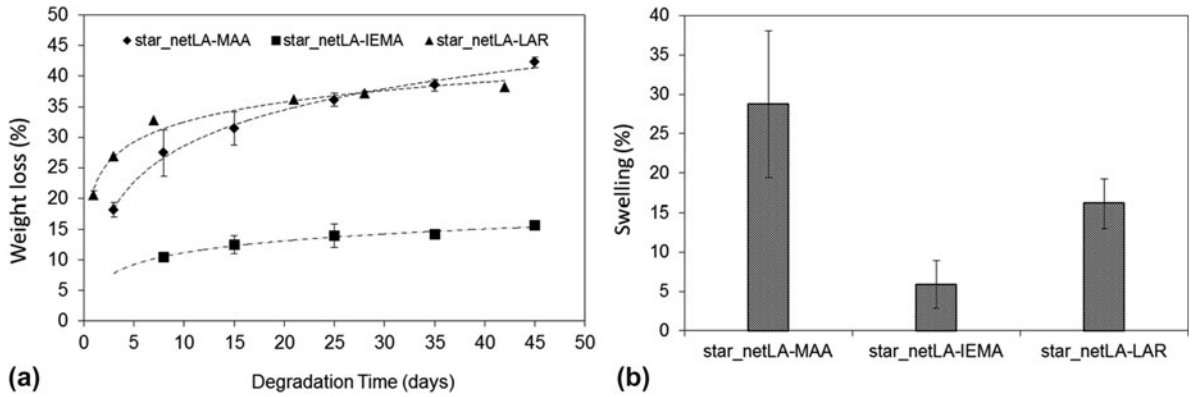


FIG. 3. Films' (1 mm thick) weight loss during its incubation in PBS at 37 °C (logarithmic adjust line is shown)—(a). Water uptake for the synthesized membranes at room temperature—(b). In both graphs, data are expressed as mean ±SME (n = 3).

https://doi.org/10.1557/jmr.2018.73 Published online by Cambridge University Press

that in vivo degradation is much faster than in vitro.[32] In fact, Mason et al.[33] reported that the degradation rate for poly(D,L-lactide) (PLA) in plasma was double than that in a buffer or water at 37 °C and attributed this to an increase in chain mobility due to lipid components in the plasma which are absorbed by PLA. Therefore, the degradation of the prepared materials is expected to be much higher when in vivo.

Comparing films synthesized with prepolymers with a different architecture (linear versus star), it may be stated that, in general, the linear oligomers impart lower hydrolytic instability than branched ones, and this may be due to a lower crosslinking density.[22]

Among the L-lactic acid-based functional films manufactured, the star-shaped networks exhibited higher swelling rate (Table I) compared to the linear materials (22.4, 10.3, and 6.6% for the films prepared with functional monomer MAA, LAR, and IEMA, respectively[18–20]). This evidence allows foreseeing the ability to tailor the degradation rates of a material from the very first step of the production process and accordingly to a particular application. This is a very advantageous feature of these new products as compared to the non-biodegradable materials currently available.

D. Thermal properties

The DMTA measurements were carried out in the Single cantilever bending mode, and in multifrequency, to allow a ready identification of the α-transition. The traces obtained at 1 Hz are shown in Fig. 4 and the glass transition temperatures, taken from the tan δ, are recorded in Table I.

All crosslinked networks depicted glass transition temperatures lower than physiological temperature, therefore satisfying an important requirement for the photocuring process. Furthermore, these results corroborate the flexible structures of all produced films.

Comparing the T_g of branched polymers (Table I), these are slightly different confirming, once more, the influence of the functional agent.

E. Cytotoxicity

All efforts in producing novel functional materials based on L-lactic acid oligomers would not be valued or even considered by the biomaterials market if they failed to be cell-compatible materials. The contact of cells with materials should favor their adhesion, proliferation, and growth, and the by-products resulting from their degradation must be absorbable by the living system, without eliciting any toxic effect.

Figures 5 and S1 (presented in the Supplementary Material) display the percentage of viable cells (assessed by the MTS assay) after they are seeded in contact with films for 1, 2, 3, 7, 10, and 14 days. Cells' adhesion and proliferation were also monitored using an inverted light microscope (Figs. 6 and S2). Through the comparison of the samples' results to the negative control (live cells), all films showed good biocompatibility in vitro with no significant cytotoxic effect. Nevertheless, there were slight differences mainly regarding the functionalizing comonomer. When comparing the biocompatibility results, it is worth emphasizing that cells in contact with MAA-based adhesives showed enhanced proliferation

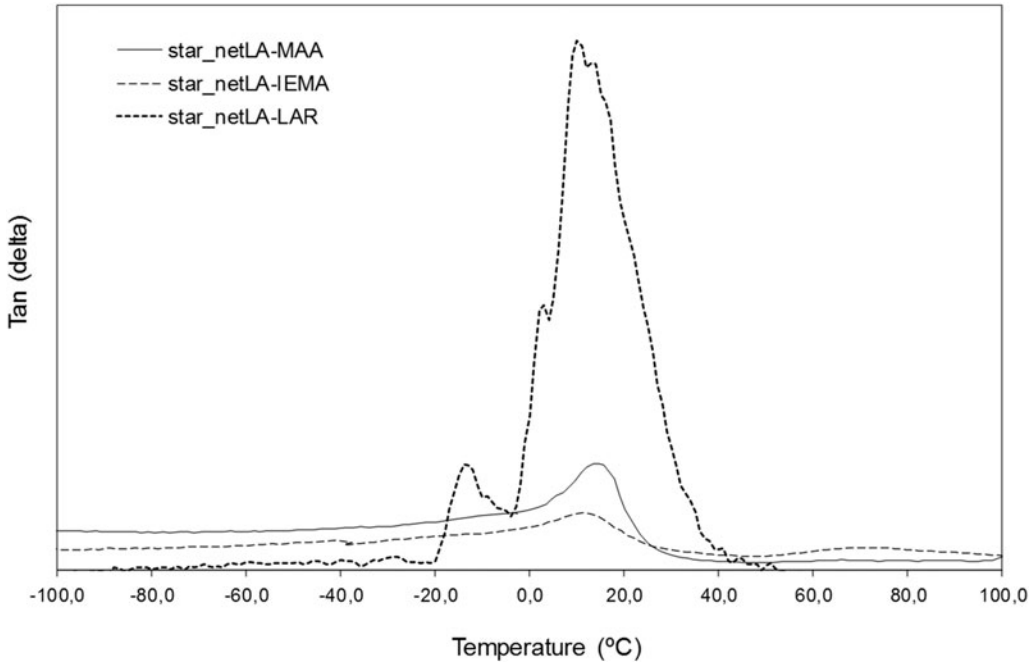


FIG. 4. The tan δ traces (at 1 Hz) for the three films registered by DMTA.

https://doi.org/10.1557/jmr.2018.73 Published online by Cambridge University Press

rates throughout the incubation period. This may be attributed to the hydrophilicity of the MAA prepolymers. As it is stated in the literature,[34] cells will adhere and grow more easily on surfaces with moderate hydrophilicity, which may therefore explain the obtained results.

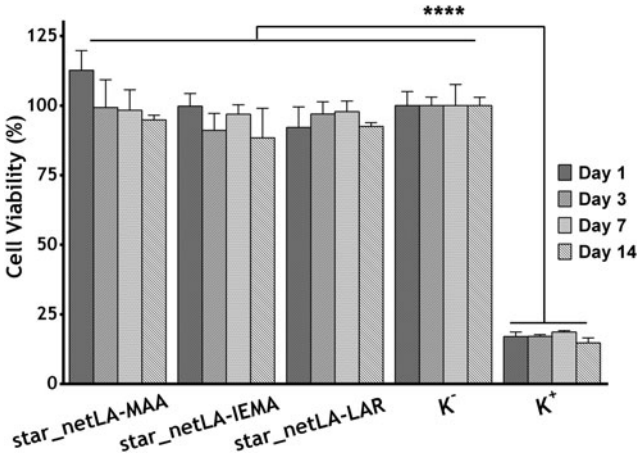


FIG. 5. Evaluation of the NHDF cells' viability after they are seeded in contact with produced membranes (star_netLA-MAA, star_netLA-IEMA, and star_netLA-LAR) for 1, 3, 7, and 14 days. K^- (negative control) and K^+ (positive control). The statistical analysis of the results was performed using one-way ANOVA with Newman–Keuls test. The result is expressed as mean ±SD ($n = 3$).

F. Qualitative evaluation of cells' viability and proliferation on the films' surface

To evaluate the cell viability and proliferation, a live/dead assay was performed after 1, 2, and 3 days post cells seeding in contact with samples. As shown in Figs. 7 and S3–S5 (as shown in the Supplementary Material), the ratio of the viable cells (green-labeled) was higher than dead (red-labeled) cells. However, NHDF cells on the surface of the star_netLA-MAA film reached a confluent monolayer faster than the cells on top of the other formulations, thus displaying a higher proliferative potential in the presence of MAA prepolymers. These findings are in accordance with the previous data obtained in cytotoxic assay.

G. Evaluation of cell adhesion on the films' surface

Beyond materials biocompatibility, it is desirable that the biomaterials' surface promotes cell adhesion, proliferation, migration, and extracellular matrix deposition.

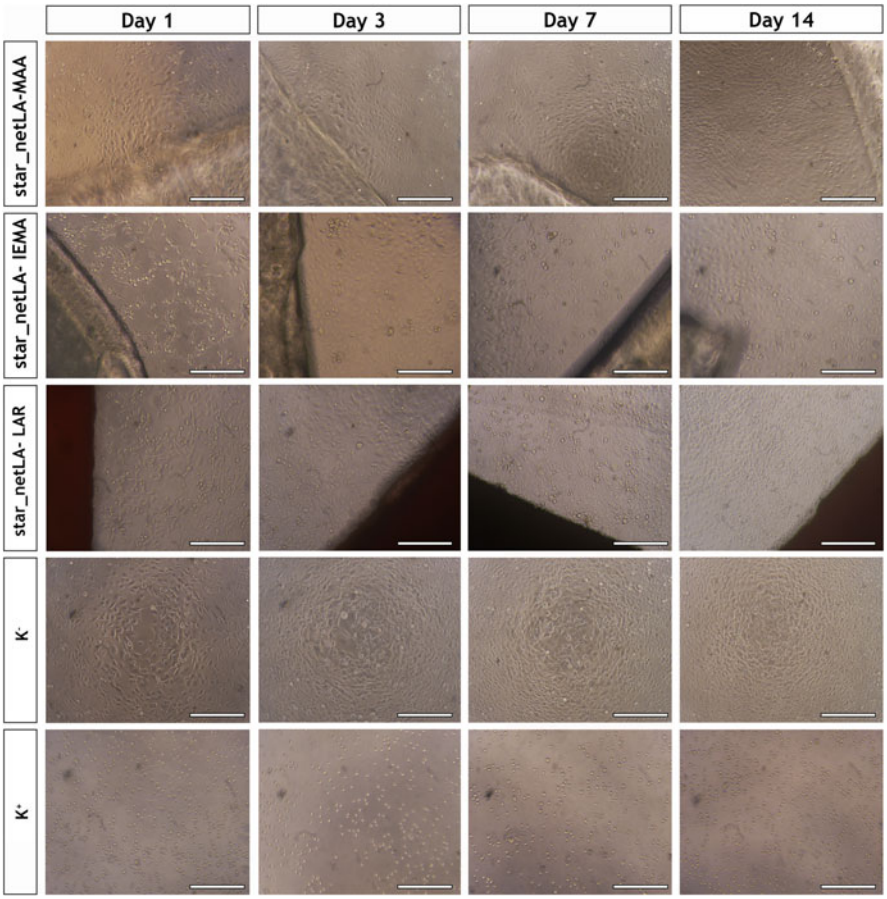


FIG. 6. Optical microscopy photographs of NHDF cells in the presence of the produced membranes after 1, 3, 7, and 14 days of incubation. K^- (negative control); K^+ (positive control). Each scale bar represents 200 μm.

https://doi.org/10.1557/jmr.2018.73 Published online by Cambridge University Press

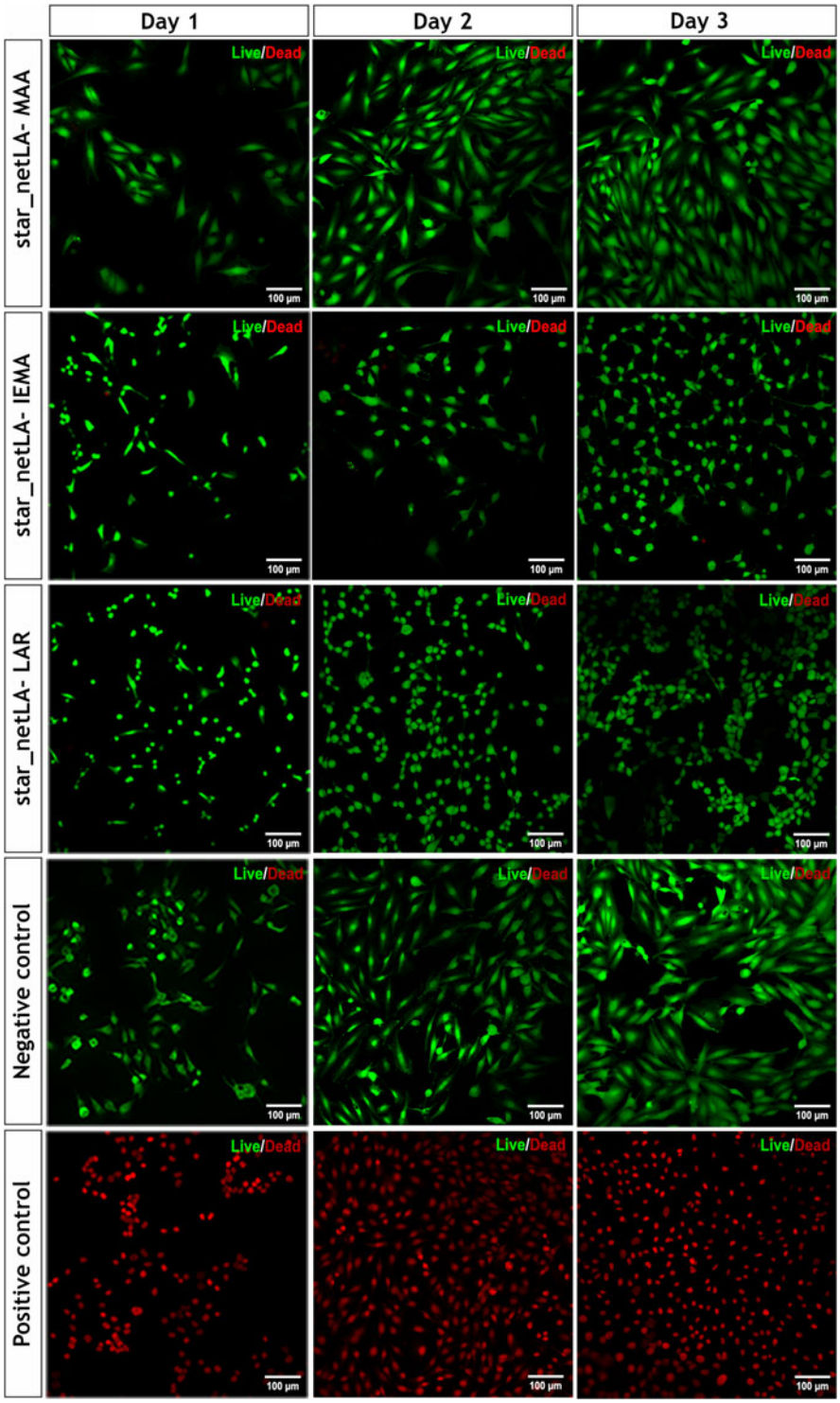


FIG. 7. Fluorescence microscopy detection of live (green-labeled) and dead (red-labeled) of the NHDF cells in contact with the produced films after 1, 2, and 3 days of being seeded in contact with the samples. The images represent the merge of two channels: Green channel (calcein AM) depicts live cells; red channel (propidium iodide) shows dead cells.

Here, films' suitability to support cell adhesion was investigated by seeding NHDFs on the surface of the films and further characterized by SEM analysis.

The hydrophilic surfaces of the produced films enhanced cell adhesion, as depicted in Fig. 8. NHDF cells attached and spread across the surface of the materials, revealing cytoplasm extensions, after 1 day of being seeded on the films' surface. After 3 days of incubation, multiple filopodia protrusions were observed, and a layer of cells started to be formed.[35]

https://doi.org/10.1557/jmr.2018.73 Published online by Cambridge University Press

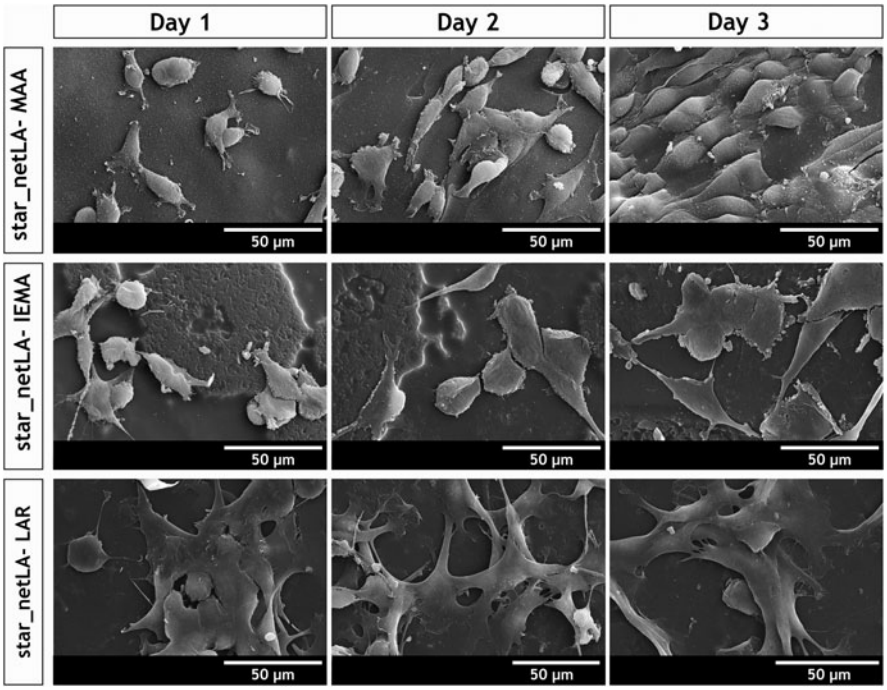


FIG. 8. SEM micrographs of NHDF cells' morphology adhered on the surface of the different produced membranes, after 1, 2, and 3 days.

IV. CONCLUSION

As the results reveal, promising functional materials with branched architecture were successfully manufactured from a renewable monomer. The prepared materials presented a photocrosslinkable character due to the modification of the oligomers with three different acrylic functionalizing agents containing carbon double bonds. This feature allowed the preparation of films by the addition of a photoinitiator to the macromer solution previously obtained and subsequent exposure to UV light. The obtained results, namely swelling capacity, suggest that the materials are susceptible to hydrolysis and will therefore be biodegradable once applied in vivo. In addition, thermal analysis showed that the T_g values of the films were low ensuring their flexibility at physiological and room temperature. Biocompatibility in vitro studies highlighted the biocompatible and bioadhesive character of the materials. Thus, all the attained results point out that the herein described methodology allowed the preparation of materials suitable for biomedical applications, namely as potential photocrosslinkable bioadhesives. In near future, in vivo assays will be performed to evaluate the ability of the films to adhere to tissues.

ACKNOWLEDGMENTS

The financial support from FCT for Grant No. SFRH/BD/42245/2007 and SFRH/BPD/86338/2012 is gratefully acknowledged. Sónia P. Miguel acknowledges a Ph.D. fellowship from FCT (SFRH/BD/109563/2015). The authors would also like to thank 73100, Lda. for the financial support.

REFERENCES

1. M. Donkerwolcke, F. Burny, and D. Muster: Tissues and bone adhesives—Historical aspects. *Biomaterials* **19**, 1461 (1998).
2. A. Duarte, J. Coelho, J. Bordado, M. Cidade, and M. Gil: Surgical adhesives: Systematic review of the main types and development forecast. *Prog. Polym. Sci.* **37**, 1031 (2012).
3. M. Mehdizadeh and J. Yang: Design strategies and applications of tissue bioadhesives. *Macromol. Biosci.* **13**, 271 (2013).
4. P.J. Bouten, M. Zonjee, J. Bender, S.T. Yauw, H. van Goor, J.C. van Hest, and R. Hoogenboom: The chemistry of tissue adhesive materials. *Prog. Polym. Sci.* **39**, 1375 (2014).
5. J. Mönkäre, R. Hakala, M. Vlasova, A. Huotari, M. Kilpeläinen, A. Kiviniemi, V. Meretoja, K. Herzig, H. Korhonen, and J. Seppälä: Biocompatible photocrosslinked poly(ester anhydride) based on functionalized poly(ε-caprolactone) prepolymer shows surface erosion controlled drug release in vitro and in vivo. *J. Controlled Release* **146**, 349 (2010).
6. J.L. Ifkovits and J.A. Burdick: Photopolymerizable and degradable biomaterials for tissue engineering applications. *Tissue Eng.* **13**, 2369 (2007).
7. J. Seppälä, H. Korhonen, R. Hakala, and M. Malin: Photocrosslinkable polyesters and poly(ester anhydride)s for biomedical applications. *Macromol. Biosci.* **11**, 1647 (2011).
8. R.S. Benson: Use of radiation in biomaterials science. *Nucl. Instrum. Methods Phys. Res., Sect. B* **191**, 752 (2002).
9. C. Decker: Kinetic study and new applications of UV radiation curing. *Macromol. Rapid Commun.* **23**, 1067 (2002).
10. B. Balakrishnan, M. Mohanty, P. Umashankar, and A. Jayakrishnan: Evaluation of an in situ forming hydrogel wound dressing based on oxidized alginate and gelatin. *Biomaterials* **26**, 6335 (2005).

https://doi.org/10.1557/jmr.2018.73 Published online by Cambridge University Press

11. W. Dong-An, S. Varghese, B. Sharma, I. Strehin, S. Fermanian, J. Gorham, D.H. Fairbrother, B. Cascio, and J.H. Elisseeff: Multifunctional chondroitin sulphate for cartilage tissue-biomaterial integration. *Nat. Mater.* **6**, 385 (2007).
12. A. Serrero, S. Trombotto, Y. Bayon, P. Gravagna, S. Montanari, and L. David: Polysaccharide-based adhesive for biomedical applications: Correlation between rheological behavior and adhesion. *Biomacromolecules* **12**, 1556 (2011).
13. P. Ferreira, J. Coelho, and M. Gil: Development of a new photocrosslinkable biodegradable bioadhesive. *Int. J. Pharm.* **352**, 172 (2008).
14. C.E. Brubaker and P.B. Messersmith: Enzymatically degradable mussel-inspired adhesive hydrogel. *Biomacromolecules* **12**, 4326 (2011).
15. P. Kord Forooshani and B.P. Lee: Recent approaches in designing bioadhesive materials inspired by mussel adhesive protein. *J. Polym. Sci., Part A: Polym. Chem.* **55**, 9 (2017).
16. L. Xiao, B. Wang, G. Yang, and M. Gauthier: Poly(lactic acid)-based biomaterials: Synthesis, modification and applications. In *Biomedical Science, Engineering and Technology*, D.N. Ghista, ed. (InTech, Rijeka, Croatia, 2012); p. 248.
17. X. Zheng, Y. Wang, Z. Lan, Y. Lyu, G. Feng, Y. Zhang, S. Tagusari, E. Kislauskis, M.P. Robich, and S. McCarthy: Improved biocompatibility of poly(lactic-*co*-glycolic acid) and poly-L-lactic acid blended with nanoparticulate amorphous calcium phosphate in vascular stent applications. *J. Biomed. Nanotechnol.* **10**, 900 (2014).
18. D. Marques, J. Santos, P. Ferreira, T. Correia, I. Correia, M. Gil, and C. Baptista: Photocurable bioadhesive based on lactic acid. *Mater. Sci. Eng. C* **58**, 601 (2016).
19. D.S. Marques, J.M. Santos, P. Ferreira, T.R. Correia, I.J. Correia, M.H. Gil, and C.M. Baptista: Functionalization and photocuring of an L-lactic acid macromer for biomedical applications. *Int. J. Polym. Mater. Polym. Biomater.* **65**, 497 (2016).
20. J. Santos, D. Marques, P. Alves, T. Correia, I. Correia, C.M. Baptista, and P. Ferreira: Synthesis, functionalization and characterization of UV-curable lactic acid based oligomers to be used as surgical adhesives. *React. Funct. Polym.* **94**, 43 (2015).
21. A.S. Karikari, B.D. Mather, and T.E. Long: Association of star-shaped poly(D,L-lactide)s containing nucleobase multiple hydrogen bonding. *Biomacromolecules* **8**, 302 (2007).
22. R.A. Hakala, H. Korhonen, and J.V. Seppälä: Hydrolysis behaviour of crosslinked poly(ester anhydride) networks prepared from functionalised poly(ε-caprolactone) precursors. *React. Funct. Polym.* **73**, 11 (2013).
23. A.O. Helminen, H. Korhonen, and J.V. Seppälä: Structure modification and crosslinking of methacrylated polylactide oligomers. *J. Appl. Polym. Sci.* **86**, 3616 (2002).
24. S. Marrian: The chemical reactions of pentaerythritol and its derivatives. *Chem. Rev.* **43**, 149 (1948).
25. D. Åkesson, M. Skrifvars, J. Seppälä, M. Turunen, A. Martinelli, and A. Matic: Synthesis and characterization of a lactic acid-based thermoset resin suitable for structural composites and coatings. *J. Appl. Polym. Sci.* **115**, 480 (2010).
26. A.S. Karikari, W.F. Edwards, J.B. Mecham, and T.E. Long: Influence of peripheral hydrogen bonding on the mechanical properties of photo-cross-linked star-shaped poly(D,L-lactide) networks. *Biomacromolecules* **6**, 2866 (2005).
27. A. Vieira, P. Ferreira, J. Coelho, and M. Gil: Photocrosslinkable starch-based polymers for ophthalmologic drug delivery. *Int. J. Biol. Macromol.* **43**, 325 (2008).
28. J. Almeida, P. Ferreira, A. Lopes, and M. Gil: Photocrosslinkable biodegradable responsive hydrogels as drug delivery systems. *Int. J. Biol. Macromol.* **49**, 948 (2011).
29. S. Dinescu, B. Galateanu, M. Albu, A. Cimpean, A. Dinischiotu, and M. Costache: Sericin enhances the bioperformance of collagen-based matrices preseeded with human-adipose derived stem cells (hADSCs). *Int. J. Mol. Sci.* **14**, 1870 (2013).
30. S.P. Miguel, M.P. Ribeiro, H. Brancal, P. Coutinho, and I.J. Correia: Thermoresponsive chitosan–agarose hydrogel for skin regeneration. *Carbohydr. Polym.* **111**, 366 (2014).
31. H.K. Makadia and S.J. Siegel: Poly lactic-*co*-glycolic acid (PLGA) as biodegradable controlled drug delivery carrier. *Polymers* **3**, 1377 (2011).
32. X. Ma, S. Oyamada, T. Wu, M.P. Robich, H. Wu, X. Wang, B. Buchholz, S. McCarthy, C.F. Bianchi, and F.W. Sellke: In vitro and in vivo degradation of poly(D,L-lactide-*co*-glycolide)/amorphous calcium phosphate copolymer coated on metal stents. *J. Biomed. Mater. Res., Part A* **96**, 632 (2011).
33. N. Mason, C. Miles, and R. Sparks: Hydrolytic degradation of poly DL-(Lactide). In *Biomedical and Dental Applications of Polymers*, Vol. **14**, C.G. Gebelein and F.F. Koblitz, eds. (Polymer Science and Technology, Plenum, New York, 1981); p. 279.
34. E. Vidovic: The development of bioabsorbable hydrogels on the basis of polyester grafted poly(vinyl alcohol). Ph.D. thesis, Rheinisch-Westfälischen Technischen Hochschule Aachen, Aachen, Germany, 2006.
35. S.I. Fraley, Y. Feng, R. Krishnamurthy, D-H. Kim, A. Celedon, G.D. Longmore, and D. Wirtz: A distinctive role for focal adhesion proteins in three-dimensional cell motility. *Nat. Cell Biol.* **12**, 598 (2010).

Supplementary Material

To view supplementary material for this article, please visit https://doi.org/10.1557/jmr.2018.73.

https://doi.org/10.1557/jmr.2018.73 Published online by Cambridge University Press